Investigation of Delamination Modeling Capabilities for Thin Composite Structures in LS-DYNA®

S.A. Muflahi, G. Mohamed*, S.R. Hallett

Advanced Composites Centre for Innovation and Science (ACCIS), Faculty of Engineering, University of Bristol, Queen's Building, Bristol, BS8 1TR, United Kingdom
**Email: G.Mohamed@bristol.ac.uk*

Abstract

*Predictive capabilities to simulate the initiation and propagation of delamination in thin composite laminates have been investigated. Different element formulations (3D solids, 2D shells, and 3D thick shells), cohesive fracture models (commercially available in LS-DYNA 971 v6.1 and *USER_DEFINED constitutive behavior) and stacking procedures have been applied to representative composite models of increasing complexity to demonstrate their response, delamination failure modes and computational efficiency. It has been shown that stacks of 2D shell elements with nodal offsets with a user-defined constitutive model for cohesive elements can retain many of the necessary predictive attributes of delamination dominated failure while providing superior computational efficiency and flexibility required for industrial component scale design.*

Introduction

Employing robust and computationally efficient tools during the design phase of composite components for flaw and damage tolerance is of benefit to the aerospace sector. Currently, cohesive elements can be used in commercial finite element software packages to predict the initiation and propagations of delaminations. These elements are governed by a strength-based initiation criteria followed by a fracture mechanics criterion for crack propagation. The softening law, which behaves according to a mixed-mode bi-linear traction separation law requires very refined meshes ahead of the crack tip for stable crack growth, with typical requirement of three elements within the fracture process zone [1]. For brittle carbon fiber-reinforced plastics, a typical cohesive length of ~ 0.1 mm is required, which can dramatically increase the CPU-time. However, this requirement can be artificially relaxed by reducing the interfacial strength whilst keeping the fracture toughness constant to obtain larger cohesive zone lengths. Since these elements represent the 'zero-thickness' bond between each adjacent plies, additional pre-processing steps are required to implement them. When undertaking finite element modeling of composite components at an industrial scale it is not feasible to include zero-thickness interface elements at individual ply boundaries due to mesh size limitations and geometrical complexity. There is thus an incompatibility between the required length scale to accurately predict delamination and the required mesh size used for industrial components.

The purpose of this paper is to explore different methods for the construction and prediction of delaminations in composite laminates using both in-built and user-defined constitutive laws and element formulations in LS-DYNA v971 r6.10 [2,3]. A pragmatic approach was taken to review at an elementary level the accuracy, robustness, and computationally efficiency of these different methods, assessed in terms of transmittance of forces and the ability to capture the mode I, II and mixed-mode behavior. This work forms part of a wider initiative to explore more flexible means of exploring component level design/failure space to realize the full potential of composite structural materials and geometries.

Modeling Methodology

Element formulation

Due to the inherent orthotropy and 3-dimensional nature of fiber-reinforced composite materials, accurate representation of the composite plies requires both a suitable constitutive law and element formulation. In LS-DYNA various approaches are available to describe the orientation, spatial distribution (thickness) and constitutive behavior of multi-layered composite materials. A summary of the most relevant element formulations for composite applications is given in Fig. 1 and Table 1.

For thin walled composite structures, the large aspect ratio of the structure (in the order of hundreds) compared to the laminate thickness (mm) implies that whilst the structural system is globally three-dimensional, plane stress approximations apply. In such applications, 2D shell elements are commonly used in which each layer can be assumed to be in a state of plane stress, with all through-thickness normal and shear components of the stress tensor σ_{13}, σ_{23}, σ_{33} are assumed to be negligible in comparison with their in-plane counterparts σ_{11}, σ_{22}, σ_{12}. In LS-DYNA, by invoking the *PART_COMPOSITE or *INTEGRATION_SHELL card, it is possible to assign different material properties, fiber orientation, and variable thickness within one layer of multiple integration points. In Fig. 1a, 2D shells 'with offsets', illustrates the use of *ELEMENT_SHELL_OFFSET card to offset distance from the plane of the nodal points to the references surface of the shell in the direction of its normal vector.

The planar assumption required for using shell elements in composite structures must be used with caution and several specific conditions must be considered (geometry, nature of boundary and loading conditions, and material response). For example, in the limiting case of thick composite laminates, for which the aspect ratio of the laminate length/width with respect to the overall laminate thickness approaches unity, clearly precludes the use of shell elements since the inter-laminar through-thickness stress tensor components are no longer negligible. In such cases, 3D solid elements are preferable but using one solid element per layer, as shown in Fig. 1b, is not practical for large structures since this can lead to large number of elements and heavy CPU requirements. Alternatively, a smearing (homogenization) approach using the classical laminate theory (CLT) can be used to represent the laminate response removing the identity and material response of each layer allowing for more computationally manageable models. However, makes capturing discrete locations of damage and delamination in the through-thickness direction difficult and could result in inaccurate predictions.

The final approach which combines the computationally efficiency of 2D shell elements and the three-dimensional nature of solid elements, is the 3D layered solid element, referred to from herein as thick shells. These elements are 8-node continuum layered solid elements which use one integration point per layer and any number of integration points through the thickness.

Furthermore, *PART_COMPOSITE can be invoked similar to shell elements, to represent layers of different material ID, fiber orientation and thickness.

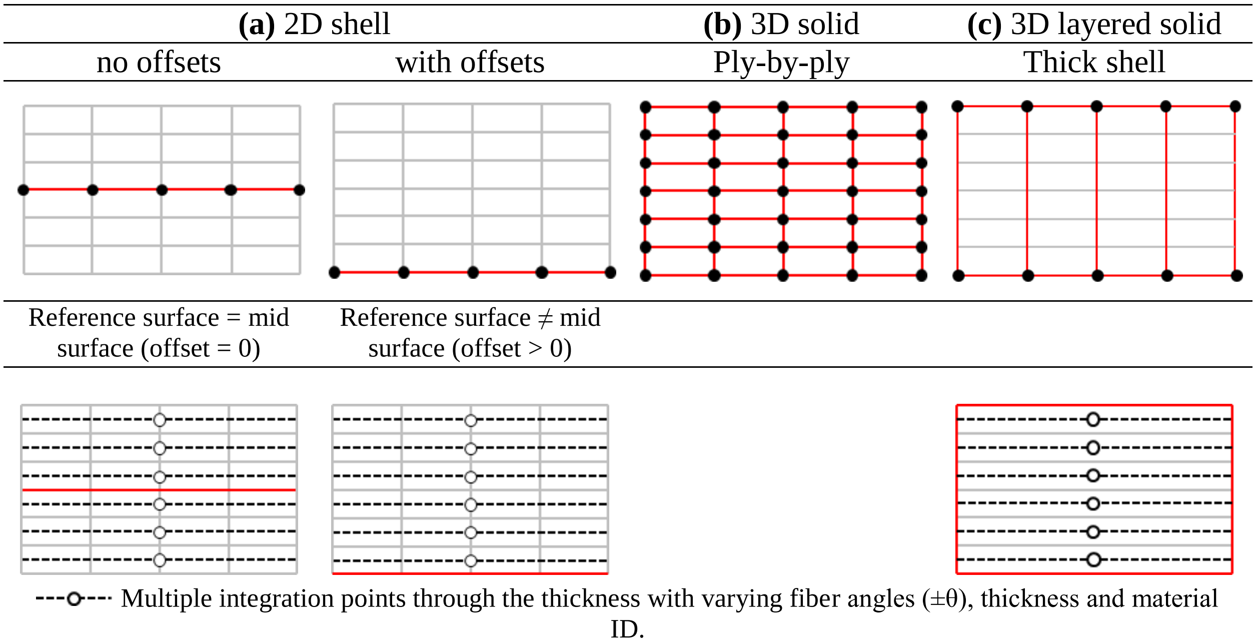

Figure 1 Available element formulations and approaches for composite structural analysis

Cohesive fracture capabilities in LS-DYNA

Table 2 provides a comprehensive, though not complete, overview of the cohesive fracture capabilities in LS-DYNA 971 r6.1 for 3-D explicit analysis [3]. Cohesive contact fracture model *CONTACT_AUTOMATIC_ONE_WAY_SURFACE_TO_SURFACE_TIEBREAK Type 9 is the Dycoss Discrete Crack Model which is governed by a linear traction separation law with quadratic mixed-mode delamination criterion and a power law (P) and Benzeggah-Kenane (B-K) damage formulation.

Type 9 can be implemented between solid elements, whereas Type 11 is an extension of Type 9 for stacked shell elements with offsets. Also included in Table 2 are four cohesive material models, MAT_138, MAT_184, MAT_185, MAT_186, with MAT_138 being a simplification of MAT_186 (restricted to linear softening)[2] and has an identical constitutive formulation to that of the DYCOSS cohesive contact models. These materials are compatible with 8-node (4-point) cohesive elements (*SECTION_SOLID Type 19/20), which can accommodate finite or zero-thickness constitutive thicknesses. Type 20 can be used with offsets shell interfaces. Finally, the last material model is a user-defined mixed-mode bi-linear cohesive fracture model as implemented by Jiang et al [4]. This material model has been extensively tested and verified for a range of loading test cases and has the added flexibility of post-processing meaningful state variables of mode-mixity, energy dissipation and damage state parameters.

Table 1 Description of element formulations available in LS-DYNA 971 v6.1; tested and reviewed in this paper

LS-DYNA element formulations

*SECTION	ELFORM: TYPE:	Description	Hourglassing
_SHELL	2	Belytschko- Tsay,	**Type 8** for Type 16 shell elements (activates full projection warping stiffness)
	16	Fully integrated shell element (very fast),	
	25	Belytschko-Tsay shell with thickness stretch.	
	26	Fully integrated shell with thickness stretch	
_SOLID	1	Constant stress solid element	**Type 6** Belytschko-Bindeman
	2	Fully integrated S/R solid	
_TSHELL	1	One point reduced integration (default),	**Type 2** Flanagan-Belytschko viscous form
	2	Selective reduced 2 x 2 in plane integration.	
	3	Assumed strain 2 x 2 in plane integration	
	5	Assumed strain reduced integration	

3-Point bend models

To investigate the accuracies and attributes of the aforementioned element formulations in terms of stiffness only and cohesive fracture models, simply supported three-point bend models, from which analytical solutions are available, were devised and tested under displacement control conditions. Figure 2 shows a schematic of the three-point bend (3PB) model where L, h and b refer to the beam length, thickness and width, respectively. Three benchmark cases of no delamination interface ($n=0$), single ($n=1$), and multiple ($n=3$) interfaces were considered. For simplicity, the constitutive material model was assumed to be isotropic (*MAT_ISOTROPIC), with E = 210 GPa and υ = 0.3.

The modeling methodology employed in this paper to capture single ($n=1$) and multiple ($n=3$) delamination is shown in Fig. 3. Finite thickness cohesive elements (Type 19/20) are inserted at the mid-plane between the interfaces of two continuum elements, which behave according to the mixed-mode delamination constitutive model *MAT_138_COHESIVE_MIXED_MODE, properties of which are given in Table 3. The implementation of a cohesive element between coincident (and non-coincident) layers of stacked shell elements, as shown in Fig. 3, follows two approaches; (a) offsetting the thickness of a coincident layer of shell elements relative to the bottom reference surface, or (b) taking account for the nodal thickness offset (in the case of non-coincident layers of shell elements) by applying a contact algorithm (*TIED_SHELL_EDGE_TO_SURFACE_BEAM_OFFSET) such that kinematic and interfacial continuity is enforced.

Table 2 Overview of appropriate cohesive fracture models available in LS-DYNA 971

	LS-DYNA definition	Stacked shell with offset	Stacked solid	Zero thickness capability	Initiation Criteria	Damage model
1	*CONTACT_AUTOMATIC_ ONE_WAY_SURFACE_TO _SURFACE_TIEBREAK Type 9	No	Yes	Yes	Strength (S)/ Quadratic (Q)	Power (P) & B-K law
2	*CONTACT_AUTOMATIC_ ONE_WAY_SURFACE_TO _SURFACE_TIEBREAK Type 11	Yes	No	N/A	S/Q	P/B-K
3	*MAT_138	Yes	Yes	Yes	S/Q	P/B-K
4	*MAT_184	Yes	Yes	Yes	S/Q	P
5	*MAT_185	Yes	Yes	Yes	S/Q	P
6	*MAT_186	Yes	Yes	Yes	S/Q	P
7	*MAT_USER_DEFINED_ MATERIAL_MODELS UMATXX**c** (Jiang et al.)	Yes	Yes	Yes	S/Q	P/B-K

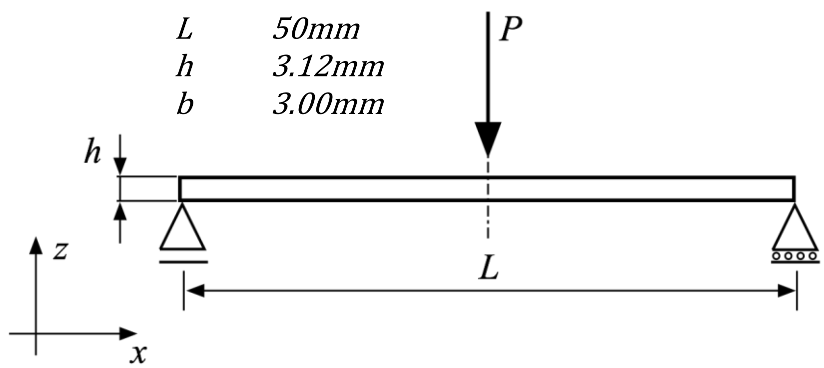

Figure 2 Three-point bend loading arrangement

Table 3 Cohesive material properties implemented in *MAT_138_COHESIVE_MIXED_MODE

K_I N/mm^3	K_{II} N/mm^3	G_{Ic} N/mm	G_{IIC} N/mm	σ_{Imax} MPa	σ_{IImax} MPa
1x10^5	1x10^5	0.26	1.002	30	60

The areal mesh density is the same for all the models but differ in the number of 3D continuum elements through the thickness. To capture accurate bending, three elements were used in the solid element test case, and, as recommend in the LS-DYNA 971 keyword manual, one and two elements were implemented for the TSHELL (Type 1/2/5) and TSHELL (Type 3), respectively[3].

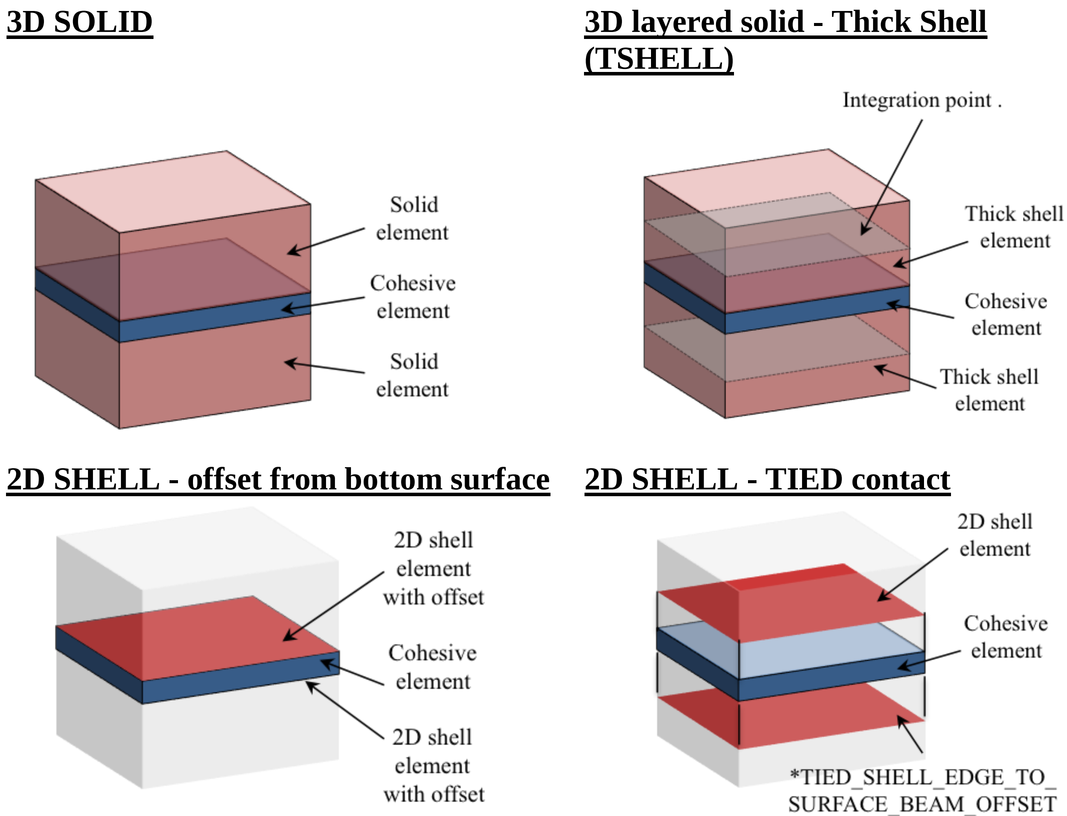

Figure 3 3-point bend models with single mid-plane interface for 2D, 3D & thick shell element formulations.

Results – 3-point bend models

An assessment of the element formulations employed in this paper is summarized in Table 4 where *n* refers to the number of delamination interfaces. For *n=0,* it is evident that all the element formulations perform reasonably well in capturing the global bending behavior and stiffness compared to the analytical beam theory solution. Although similar conclusions can be made for single and multiple delaminations, it appears that for *n=1*, employing cohesive elements between stacks of shell elements with a contact tied algorithm (2D shells – TIED_SHELL_EDGE_TO_SURFACE) can result in non-conservative results of stiffness and initiation of delamination (see Fig. 4). Clearly, the interfacial continuity in transferring translational and rotational degrees of freedom and nodal forces from the shell elements to the cohesive is not properly enforced. Further work is needed to investigate this approach in detail. In contrast, 2D elements with 'offsets' clearly perform as well as solid and thick shells. However, 2D shells models appear to over-predict the initiation of delamination. This result is not unexpected, since inter-laminar delamination is governed by out-of-plane inter-laminar shear stresses which are absent in 2D shell element formulations based on plane stress assumption. However, thick shells of type 5 with 3D stress updates perform very well in capturing the onset of delamination growth.

Based on this preliminary study, Solid Type 2, 2D shell Type 16, and Type 5 thick shells have been down selected in achieving the optimum balance in stiffness, initiation of delamination and running times and will be implemented in representative coupon fracture toughness models for further assessment.

Table 4 Summary of 3PB stiffness results obtained from different element formulations. Color criteria: red (>10% from theory, risk/not suitable), amber (<5% from theory, potential), green (< 5% from theory) and dark green (<50% and recommended)

*SECTION	ELFORM: TYPE:		Target stiffness value from beam theory	Number of interfaces (n)		
				n=0	*n=1*	*n=3*
_SOLID	1		612.29	596.32	600.92	630.20
	2		612.29	616.73	600.92	639.39
_SHELL	2	OFFSET	612.29	604.97	604.97	600.18
		*TIED	612.29	n/a	529.65	X
	16	OFFSET	612.29	611.12	611.12	607.78
		*TIED	612.29	n/a	531.15	X
	25	OFFSET	612.29	594.58	594.58	X
		*TIED	612.29	n/a	531.77	X
	26	OFFSET	612.29	563.42	563.42	n/a
		*TIED	612.29	n/a	464.24	X
_TSHELL	1		612.29	651.69	583.04	653.31
	2		612.29	651.69	583.04	X
	3		612.29	569.75	594.00	X
	5		612.29	643.04	594.00	652.10

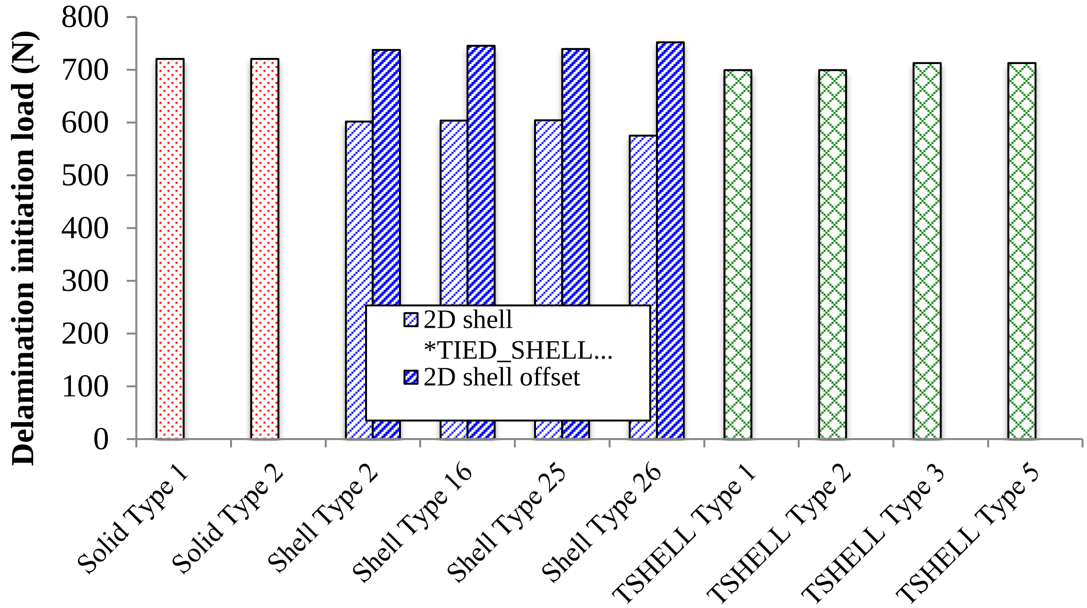

Figure 4 Summary of delamination initiation load (n=1) for different element formulations.

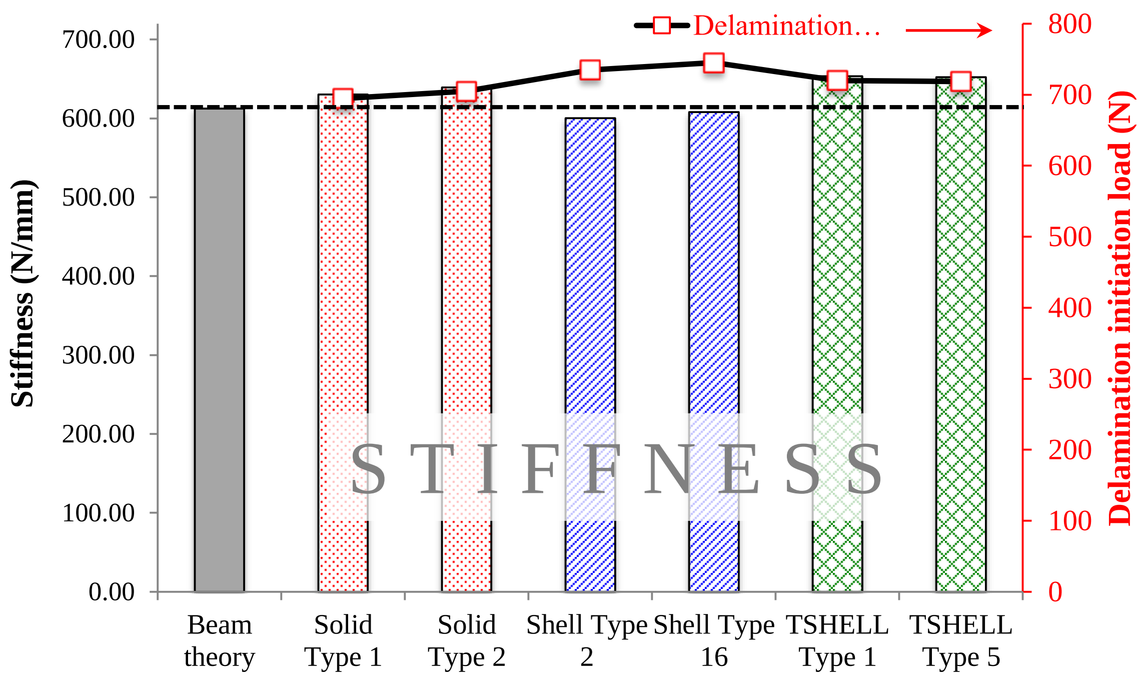

Figure 5 Summary of both the stiffness and delamination initiation load (n=3) results obtained from different element formulations with the dashed line indicating an analytical derived delamination initiation load

Fracture toughness modeling

Simple Mode I (Double Cantilever Beam – DCB), Mixed-Mode (Fixed-Ratio Mixed Mode – FRMM), and Mode II (3-point End-Notched Flexure – ENF) were performed to further evaluate the performance of cohesive fracture models, see Fig. 6. Models of 24-ply unidirectional

AS4/PEEK carbon fiber reinforced composite was simulated and compared with available beam theory solutions. The specimen length, *L*, is given in Fig. 6 and 20.0 mm wide with two, *2h*, 1.55 mm-thick arms, the latter providing a mode mixity of G_{II}/G_T = 43% for the FRMM models. The initial delamination length is a_0 = 35 mm. The material properties of the AS4/PEEK specimen are as follows: E_{11} = 120 GPa, E_{22} = E_{33} = 11 GPa, ν_{12} = ν_{13} = 0.32, ν_{23} = 0.45, G_{12} = G_{13} = 5.5 GPa, and G_{23} = 3.7 GPa[1]. The properties of the interface are given in Table 3. The average size of the continuum and cohesive elements in the direction of crack propagation is 0.5 mm.

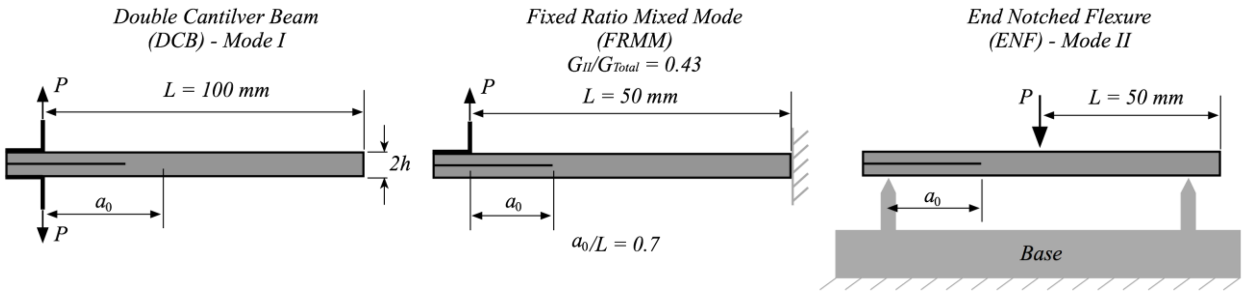

Figure 6 DCB, FRMM and ENF test specimens

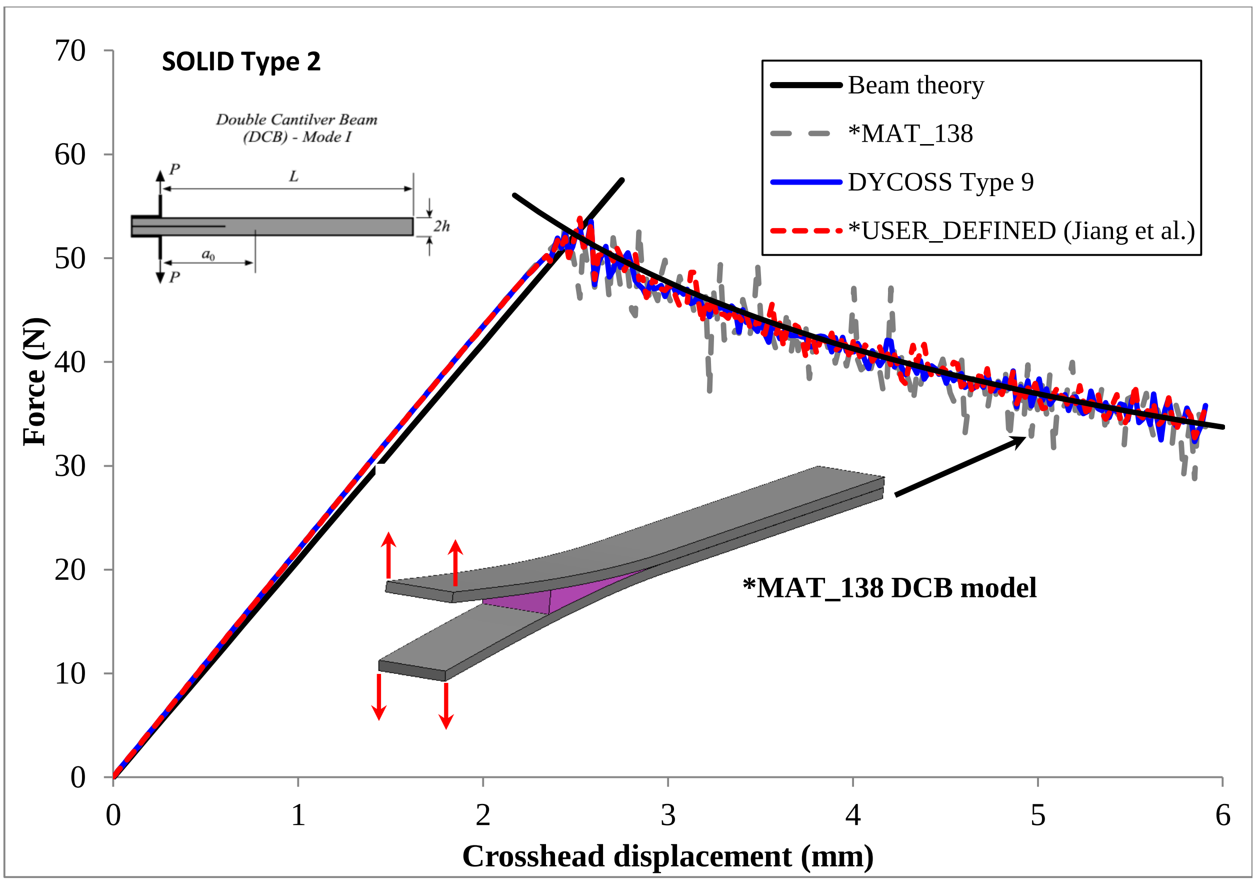

Figure 7 Predicted & analytical response of Solid Type 2 mode I DCB models

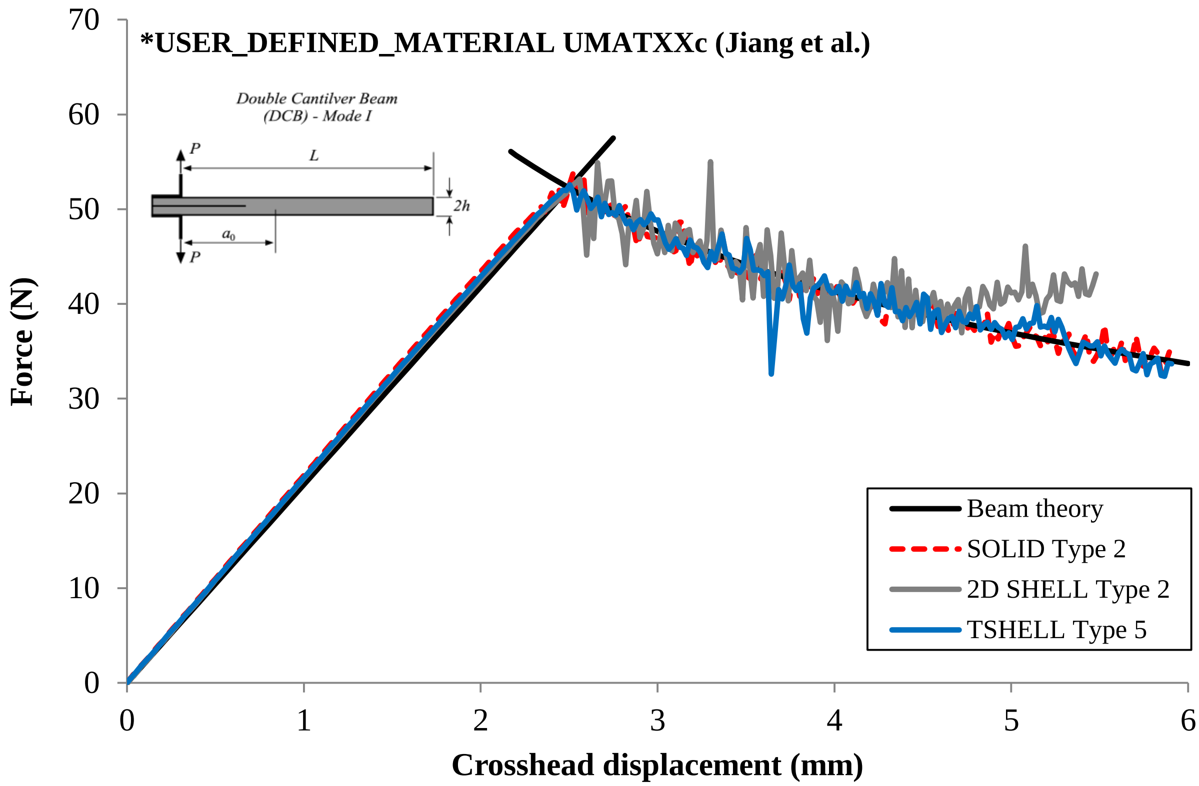

Figure 8 Predicted and analytical response of *USER_DEFINED mode I DCB models

The numerical and analytical results shown in Figs. 7-11 relate the load to the displacement of the point of load application. For mode I and II, it can be observed that excellent agreement is obtained across all element and material formulations, as shown in Figs 7/8 (mode I DCB) and Figs. 9/10 (mode II 3ENF). However, in mode II, thick shells show premature initiation of delamination followed by post-damage oscillations. This may be a result of stacking thick shells in between Type 19 8-node cohesive elements. This oscillatory behavior is further accentuated when considering mixed-mode behavior, as shown in Fig. 11, where the thick shells show large numerical instabilities.

A summary of the CPU performance (SMP LS-DYNA 971 v6.10 on Windows 7 64-bit desktop PC on 2 i-5 processors) of the different methodologies employed in the DCB simulations (similar trends can be observed in 3ENF & FRMM) is given in Fig. 12. 2D shell elements clearly offer the fastest running times, however it appears that the Type 5 TSHELL elements offer superior computational efficiency with respect to solid elements.

It is concluded from this study that Type 16 2D shell elements with *PART_COMPOSITE are robust and accurate enough in capturing both the initiation and propagation of delamination in a relatively stable manner.

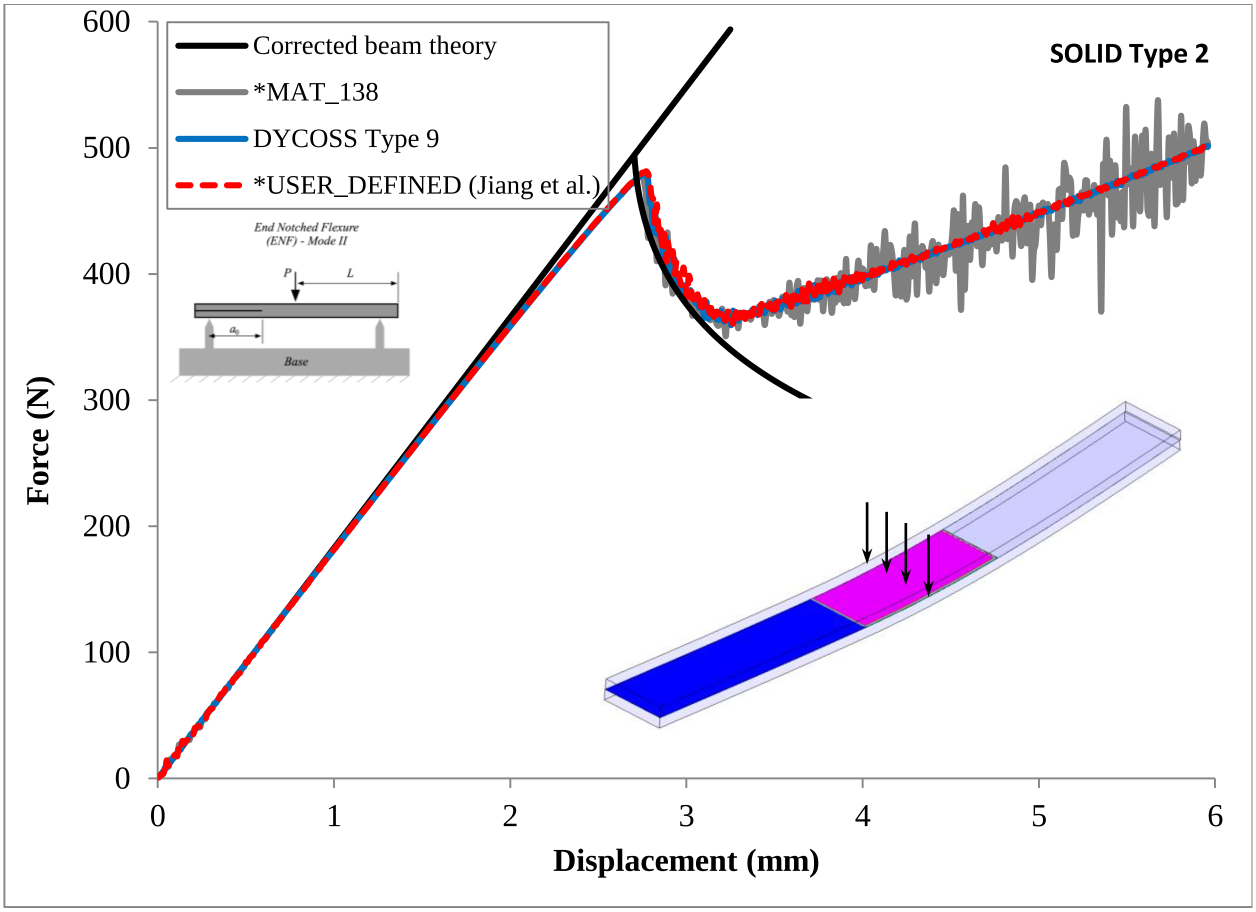

Figure 9 Predicted and analytical response of Solid Type 2 mode II 3-ENF models

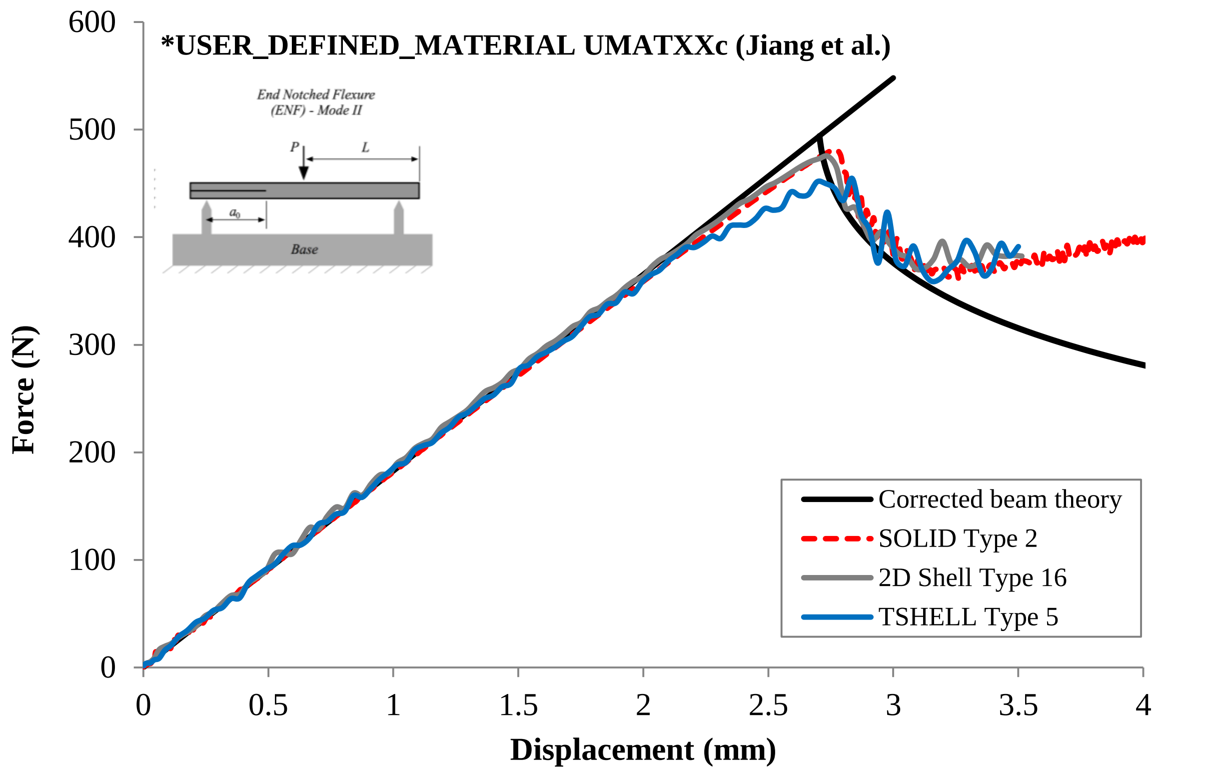

Figure 10 Predicted and analytical response of *USER_DEFINED mode II 3-ENF models.

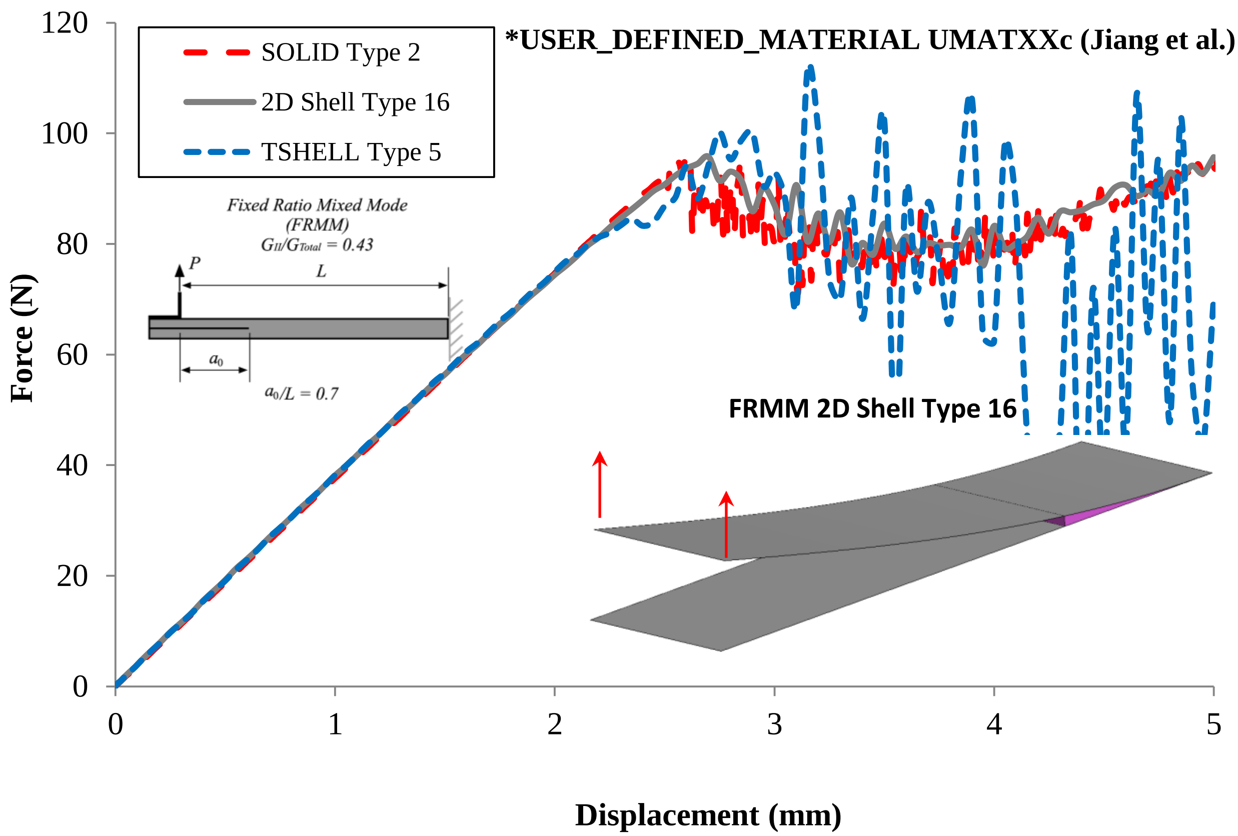

Figure 11 Predicted response of mixed-mode (43%) *USER_DEFINED FRMM simulations.

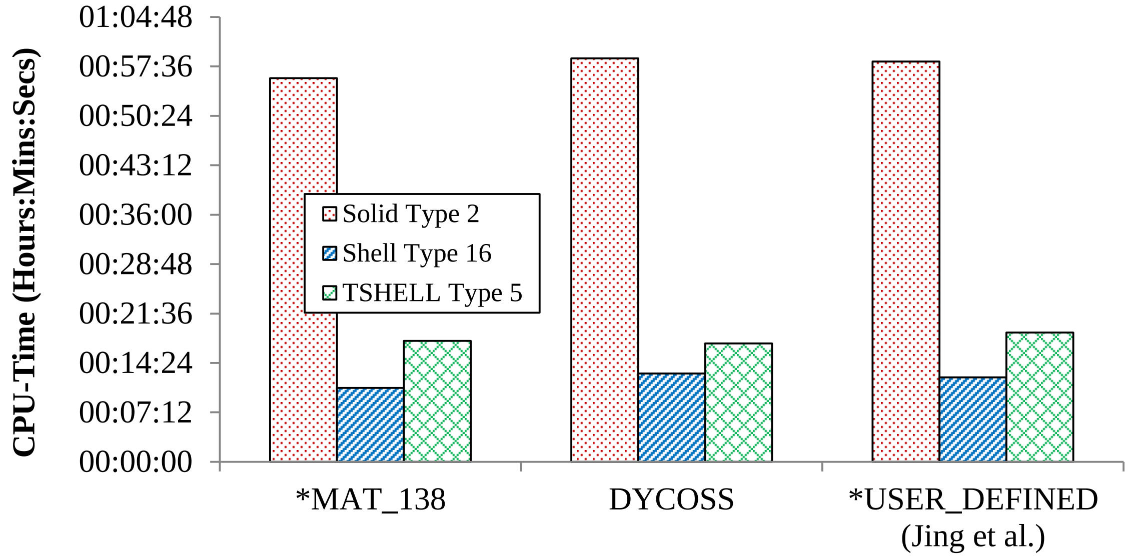

Figure 12 Summary of CPU times for all cohesive zone modeling techniques and element formulations - Mode I DCB models.

Static indentation case

Finally, the static indentation of a composite plate is simulated to verify the stability and CPU performance of a 2D stacked-shell model using *PART_COMPOSITE. A composite laminate of dimensions 150 x 100 x 4 mm laminate with a IM7/8552 quasi-isotropic lay-up $[45_2/0_2/90_2/-45_2]_{2S}$ is modeled, as shown in Fig 13, please see Ref [5] for further details.

By moving the location of a single cohesive layer through the thickness of the laminate, results are able to capture the delamination behavior of individual interfaces through the laminate, as shown in Figure 14 (a) and (b). The results match very well the delaminated area shown by the CT scans opposite. Models were analyzed on a Linux Cluster on 8 1GB CPUs and ran 15 x faster than the high fidelity model reported in Ref [5].

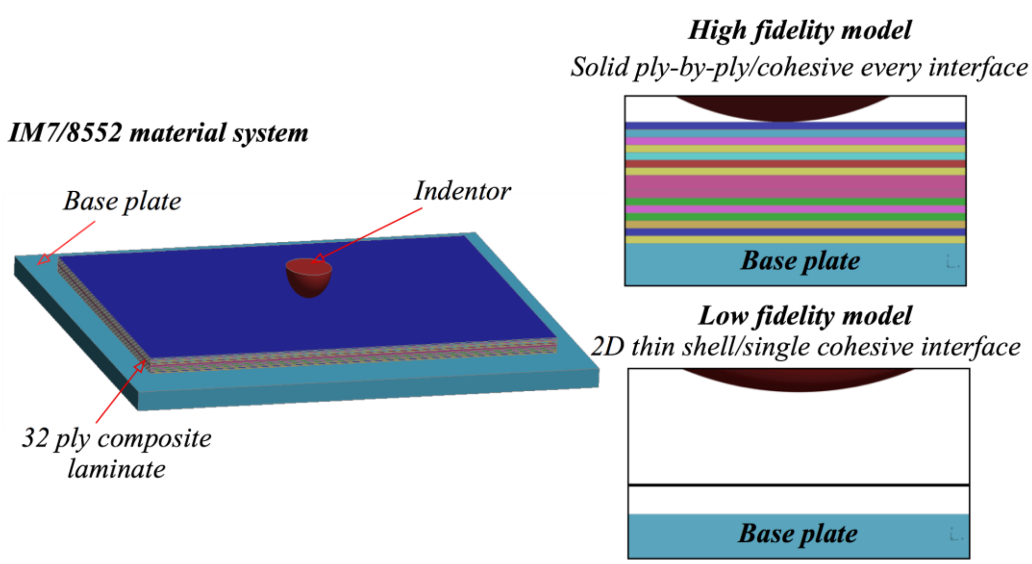

Figure 13 High and Low fidelity 3D models illustrating reduction in model complexity.

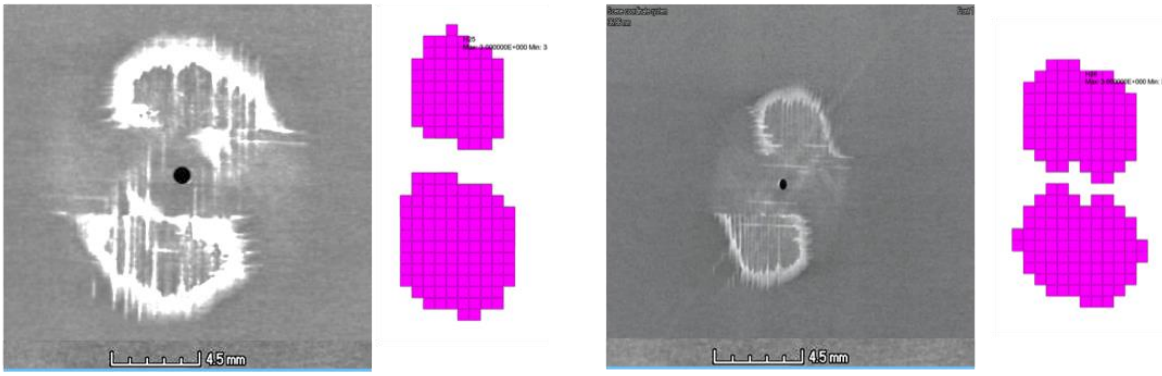

(a) Comparison of CT scan at lower 0/90 interface with 2D shell model

(b) Comparison of CT scan at upper 0/90 interface with 2D shell model

Figure 14 Comparison of delamination area of low fidelity models against CT scans

Conclusion

The predictive capabilities for modeling the initiation and growth of delamination in thin composite structures in LS-DYNA for different element types and cohesive fracture model have been presented. By considering different stacking procedures using 3D solids, 2D shells and thick shells, representative composite examples of increasing complexity were developed. It has been shown all element and cohesive fracture models are capable of delivering a sensible prediction for delamination, albeit with varying degrees of accuracy. For the best stability and accuracy in predicting the onset and propagation of delamination , it was found to use either solid or 2D shell element formulations with a USER_DEFINED cohesive material model (as demonstrated by Jiang et al.) or Dycoss (*TIEBREAK Type 9/11) cohesive contact model.

This study has also highlighted potential difficulty in using thick shells with 8-node cohesive elements (Type 19/20) for predicting delaminations in composite laminates. Instability during the propagation of delamination and severe through-thickness hourglassing are potential issues, which could hinder their use in such applications. This is a topic of further investigation.

Acknowledgements

The authors would like to acknowledge Rolls-Royce plc for the support of this research through the Composites University Technology Centre (UTC) at the University of Bristol, UK.

References

[1] Harper PW, Hallett SR. Cohesive zone length in numerical simulations of composite delamination. Eng Fract Mech 2008;75:4774–92.

[2] LSTC. LS-DYNA Keyword User's Manual Volume II Material Models. 2012.

[3] LSTC. LS-DYNA Keyword Manual Volume I. 2012.

[4] Jiang W, Hallett S. A concise interface constitutive law for analysis of delamination and splitting in composite materials and its application to scaled notched tensile specimens. Int J Numer Methods Eng 2007;69:1982–95.

[5] Sun XC, Hallett SR. Investigation of Key Damage Mechanisms in Compression After Impact/Indentation Loading. IV ECCOMAS Themat. Conf. Mech. Response Compos., 2013.